Acta Cryst. (1994). A**50**, 376–383

The Use of Sayre's Equation in Real Space

BY TOMOHIRO SATO

Shionogi Research Laboratories, Shionogi & Co. Ltd, Fukushima-ku, Osaka 553, *Japan*

(*Received* 22 *October* 1993; *accepted* 25 *November* 1993)

Abstract

A method is described for minimizing a least-squares residual to Sayre's equation as a function of electron densities under the constraints that each of the observed structure factors is strictly compatible with the densities, *i.e.* $|F_{\mathbf{h}}| - |F_{\mathbf{h}}^{\rm obs}| = 0$. By evaluation of the residual in real space using fine grid sizes, the method enables one to obtain density maps of atomic resolution even with low-resolution data. Numerical calculations have been made at various resolutions for the crystal structure of a small molecule containing only C, N, O and H atoms. It has been found that the residual can be used as a good figure of merit when the resolution of the observed diffraction data is higher than 1.5–1.8 Å. With 2.0 Å data, however, several unusual structures whose residuals are lower than that of the correct structure have been found. Their existence may indicate a limitation inherent in direct methods based on the principle of 'atomicity' in general.

Introduction

The diffraction data obtainable from a crystal are in general never sufficient to determine uniquely the electron-density distribution of the crystal structure, that is, an infinite number of density maps can be compatible with the observed data. Therefore, in order to select the correct one, it is necessary to impose additional physical or chemical restrictions on the densities. In usual structure refinements, this requirement is fulfilled by the use of atomic scattering factors tabulated from quantum-mechanical calculations. These refinements, however, are possible only with knowledge of the approximate positions of atoms. Hence, we need methods that can produce interpretable density maps without knowledge of atomic positions, notorious probabilistic direct methods [for a review see Woolfson (1987)] being such examples. In developing such a method, there are three remarks we should keep in mind: (i) The method should provide a means of selecting a single 'best' map out of many possible ones. This can be done most directly by using variational techniques and maximizing or minimizing a certain function of electron densities or phases. (ii) The method should introduce sufficient restrictions into the densities. When variational techniques are used, this amounts to inventing a suitable function. (iii) It is necessary to examine whether the 'best' map thus obtained corresponds to the correct structure.

Probabilistic direct methods aim to maximize the probability that observed structure factors have a certain combination of phase angles. Although the probability calculations are based on the 'atomicity' of crystal structures, what restrictions the methods in turn impose on electron densities are not well known. The maximum-entropy method (*e.g.* Livesey & Skilling, 1985) maximizes the Jayne/Shannon entropy and provides the most unbiased, in the sense of information theory, estimation of electron densities; but, again, the restrictions the method imposes on densities are not well known except that it makes density maps everywhere positive and smooth. Sayre (1972) developed a variational method in which a least-squares residual to Sayre's equation (Sayre, 1952) is minimized. This method has the potential to produce a density map such as is required in that all peaks have the shape compatible with a given atomic scattering factor. Although this would be possible for hypothetical structures consisting solely of identical atoms, we could expect that the exceptionally strong restriction on the densities may also be useful for more realistic structures containing heterogeneous atoms. Indeed, previous calculations based on Sayre's equation have achieved reasonable success in the field of small molecules (Krabbendam & Kroon, 1971; Navaza, 1986; Debaerdemaker, Tate & Woolfson, 1988) and macromolecules (Hoppe & Gassman, 1964; Barrett & Zwick, 1971; Sayre, 1974; Cutfield, Dodson, Dodson, Hodgkin, Isaacs, Sakabe & Sakabe, 1975; Zhang & Main, 1990; Woolfson & Yao, 1990). The present study attempts to enhance Sayre's variational method.

Sayre's equation expresses that, when a crystal structure consists only of identical resolved atoms, the electron densities ρ and their squares can be related to each other by a function of the scattering factor of the atom:

$$\rho - \psi * \rho^2 = 0, \qquad (1)$$

where the symbol $*$ denotes a convolution and ψ is

ISSN 0108-7673

the Fourier transform of Ψ; $\Psi = f/(f*f)$, where f and $f*f$ stand for the scattering factors of the atom and of the density-squared atom, respectively. By transforming (1), we obtain a more familiar form of Sayre's equation in reciprocal space as

$$F_{\mathbf{h}} - (1/V)\Psi_{\mathbf{h}}\sum_{\mathbf{k}} F_{\mathbf{k}}F_{\mathbf{h}-\mathbf{k}} = 0. \quad (2)$$

The two forms are in principle equivalent but it should be noted that, when the structure factors used in (2) are limited to observed ones, (2) is a poor approximation because the summation it contains involves structure factors outside the observed limit. On the other hand, (1) can be evaluated to any desired accuracy if fine enough grid sizes are employed. Furthermore, the use of (1) enables us to use fully the information of the atomic scattering factor contained in ψ, while in the case of (2) the use is limited by the resolution of the observed data.

In view of this, another method has been developed for minimizing the least-squares residual to Sayre's equation. This method is in principle the same as Sayre's method but differs in several details: (i) The residual is evaluated in real space using fine grid sizes. (ii) The residual is minimized as a function of densities rather than phases under the constraints that each of the observed structure factors is strictly compatible with the densities. (iii) To reduce the effects of heterogeneous atoms, observed structure factors are modified so as to conform to an averaged Gaussian atom. With these modifications, the present method acquires a capability of obtaining a density map of atomic resolution even with low-resolution data. Numerical results are presented that demonstrate how the present method works at various resolutions.

Sayre's equation in the form of (1) has already been used in different contexts (Navaza, 1986; Main, 1990). Some modifications have been proposed that make Sayre's equation in the form of (2) more usable (Barrett & Zwick, 1971; Sayre, 1972, 1975; Shiono & Woolfson, 1991). Hoppe (1963) used a least-squares residual different from the one used by Sayre (1972).

Method

Consider a unit cell divided into equal pixels, with $\rho_{\mathbf{x}}$ being the average electron density of the pixel located at $\mathbf{x}$. (The same notation is also used for other types of densities.) Structure factors are calculated as $F_{\mathbf{h}} = |F_{\mathbf{h}}| \exp i\varphi_{\mathbf{h}} = (V/N)\sum_{\mathbf{x}}\rho_{\mathbf{x}} \exp(2\pi i\mathbf{h}\cdot\mathbf{x})$, where V and N denote the cell volume and the number of pixels, respectively. Then, the minimum of a least-squares residual to Sayre's equation is found:

$$Q = (V/2N)\sum_{\mathbf{x}}(\rho_{\mathbf{x}} - \overline{\rho}_{\mathbf{x}})^2 \quad (3)$$

under the constraints

$$g_{\mathbf{h}} = |F_{\mathbf{h}}| - |F_{\mathbf{h}}^{\text{obs}}| = 0, \quad (4)$$

where $\overline{\rho} = \psi * \rho^2$ and $\mathbf{h}$ comprises the set of reflections used. According to a constrained minimization method in general use (Hestenes, 1969; Ichikawa, 1975), solutions to the present problem may be obtained by minimizing the measure

$$H = Q - \sum_{\mathbf{h}}\lambda_{\mathbf{h}} g_{\mathbf{h}} + (w/2)\sum_{\mathbf{h}} g_{\mathbf{h}}^2 \quad (5)$$

as a function of Lagrange multipliers $\lambda_{\mathbf{h}}$ and densities, provided that the positive constant w is sufficiently large. This minimization may proceed as follows. First, with $\lambda_{\mathbf{h}}$ kept at the current values, H is minimized with respect to $\rho_{\mathbf{x}}$. This is done pixel-wise by the method of steepest descent, using the derivative

$$\frac{N}{V}\frac{\partial H}{\partial \rho_{\mathbf{x}}} = \rho_{\mathbf{x}} - \overline{\rho}_{\mathbf{x}} - 2\rho_{\mathbf{x}}\hat{\rho}_{\mathbf{x}} - \sum_{\mathbf{h}}[\lambda_{\mathbf{h}} + w(|F_{\mathbf{h}}^{\text{obs}}| - |F_{\mathbf{h}}|)] \times \exp(i\varphi_{\mathbf{h}}) \exp(-2\pi i\mathbf{h}\cdot\mathbf{x}), \quad (6)$$

where $\hat{\rho} = \psi * (\rho - \overline{\rho})$. Now, we have new estimates for $\rho_{\mathbf{x}}$ using a constant step size c_1:

$$\rho_{\mathbf{x}}^{\text{new}} = \rho_{\mathbf{x}} + c_1[\overline{\rho}_{\mathbf{x}} - \rho_{\mathbf{x}} + 2\rho_{\mathbf{x}}\hat{\rho}_{\mathbf{x}} + \rho_{\mathbf{x}}^{\lambda} + w\Delta\rho_{\mathbf{x}}], \quad (7)$$

where

$$\rho_{\mathbf{x}}^{\lambda} = \sum_{\mathbf{h}}\lambda_{\mathbf{h}} \exp i\varphi_{\mathbf{h}} \exp(-2\pi i\mathbf{h}\cdot\mathbf{x}) \quad (8)$$

and

$$\Delta\rho_{\mathbf{x}} = \sum_{\mathbf{h}}(|F_{\mathbf{h}}^{\text{obs}}| - |F_{\mathbf{h}}|) \exp i\varphi_{\mathbf{h}} \exp(-2\pi i\mathbf{h}\cdot\mathbf{x}). \quad (9)$$

It should be noticed that, when $\rho_{\mathbf{x}}$ is updated, the same must be done with $\varphi_{\mathbf{h}}$. This minimization step is repeated until convergence is obtained.

Next, we update $\lambda_{\mathbf{h}}$ by new estimates that may be obtained by comparing the right-hand side of (6), which must have already vanished in the above minimization, with the following equation that the true solution should satisfy

$$\overline{\rho}_{\mathbf{x}}^{(0)} - \rho_{\mathbf{x}}^{(0)} - 2\rho_{\mathbf{x}}^{(0)}\hat{\rho}_{\mathbf{x}}^{(0)} - \sum_{\mathbf{h}}\lambda_{\mathbf{h}}^{(0)} \exp i\varphi_{\mathbf{h}}^{(0)} \exp(-2\pi i\mathbf{h}\cdot\mathbf{x}) = 0. \quad (10)$$

Thus, we have

$$\lambda_{\mathbf{h}}^{\text{new}} = \lambda_{\mathbf{h}} + w(|F_{\mathbf{h}}^{\text{obs}}| - |F_{\mathbf{h}}|). \quad (11)$$

The whole process up to this point is then repeated. If the final convergence is obtained, (11) ensures that $|F_{\mathbf{h}}| = |F_{\mathbf{h}}^{\text{obs}}|$. Then, (7) shows that

$$\rho_{\mathbf{x}} = (\overline{\rho}_{\mathbf{x}} + \rho_{\mathbf{x}}^{\lambda})/(1 - 2\hat{\rho}_{\mathbf{x}}), \quad (12)$$

which indicates that $\rho_{\mathbf{x}}$ is equivalent to a solution obtained from the Lagrangian $L = Q - \sum_{\mathbf{h}}\lambda_{\mathbf{h}} g_{\mathbf{h}}$.

The use of many individual constraints in the form of (4) has been questioned and a way has been

proposed that uses a single 'weak' statistical constraint $\sum_{\mathbf{h}}[(|F_{\mathbf{h}}| - |F_{\mathbf{h}}^{\rm obs}|)/\sigma_{\mathbf{h}}]^2 = c$, $c \le M$, where M is the number of reflections used (Gull & Daniell, 1978; Wilkins, Varghese & Lehmann, 1983). However, the present algorithm has been successfully used for maximizing entropy under the 'strong' constraints (Sato, 1992) and notable features specific to this algorithm were discussed then.

Implementation

(*a*) *Modification of observed structure factors*

In order to reduce the effects of hetereogeneous atoms, observed structure factors are modified using the predetermined overall temperature factor $B_{\rm overall}$ and a postulated Gaussian distribution $\exp(-\overline{B}s^2)$, where $s = \sin\theta/\lambda$, as

$$|F_{\mathbf{h}}^{\rm obs}|[\exp(-\overline{B}s^2)\sum_i f_i(s=0) \Big/ \exp(-B_{\rm overall}s^2)\sum_i f_i(s)], \quad (13)$$

where f_i is the atomic scattering factor of the ith atom and the summations are taken over only C, N and O atoms. Then, the crystal structure is considered to be composed of identical atoms whose scattering factor is expressed as

$$f = \overline{A}\exp(-\overline{B}s^2), \quad (14)$$

where $\overline{A} = \sum_i f_i(s=0)/\sum_i 1$.

(*b*) *Convolutions*

The convolution involved in the calculations of $\psi * \rho^2$ and $\psi * (\rho - \hat{\rho})$ is calculated using Fourier transformation in such a way that $\psi * \rho^2 = \mathcal{F}[\Psi\mathcal{F}^{-1}(\rho^2)]$, where the symbol $\mathcal{F}$ denotes a Fourier transform and

$$\Psi = (1/\overline{A})(\overline{B}/2\pi)^{3/2}\exp(-\overline{B}s^2/2) \quad (15)$$

for the atomic scattering factor in the form of (14). When this is done, all Fourier components of $\mathcal{F}^{-1}(\rho^2)$ that can be calculated by fast Fourier transformation are considered and the grid sizes are chosen such that the ripples caused by large peaks become $\psi * \rho^2 \ge -0.002$ e Å^{-3}. It is necessary to use grid sizes of 0.20, 0.25 and 0.35 Å for $\overline{B} = 6.0$, 8.0 and 14.0 Å^2, respectively.

(*c*) *Setting up the initial densities and Lagrange multipliers*

The initial densities $\rho_{\mathbf{x}}$ are either input or calculated using a given starting set of phases as usual. The starting Lagrange multipliers $\lambda_{\mathbf{h}}$ are set to zero.

(*d*) *Constrained minimization*

Updating of $\rho_{\mathbf{x}}$ with (7) is to be repeated at most five times if shifts of $\rho_{\mathbf{x}}$ are larger than 10^{-5}. Rigorous convergence of this step is not always required for updating of $\lambda_{\mathbf{h}}$ with (11). With the process as far as the updating of $\lambda_{\mathbf{h}}$ being defined as one iteration, 250 iterations were performed in the following numerical calculations. In the very first iteration, the updating of $\rho_{\mathbf{x}}$ with (7) is repeated at most 50 times.

(*e*) *Choice of the weight w*

A weight w in the range 2–20 is used. When the constraints are rather difficult to fulfil, a larger weight is used. The step size of steepest descent is set to be $c_1 = 1/w$. The updating of $\lambda_{\mathbf{h}}$ using (11) is attenuated by multiplication by a factor of 3/4.

(*f*) *Exclusion/inclusion of incorrect reflections*

As detailed previously (Sato, 1992), the present algorithm for constrained minimization is not always convergent but may sometimes diverge. This difficulty arises from the large Lagrange multipliers that result for those reflections whose phases cannot be refined continuously. To eliminate this difficulty, the exclusion/inclusion algorithm developed for the maximum-entropy calculation is used: Those reflections for which $|\lambda_{\mathbf{h}}|/|F_{\mathbf{h}}^{\rm obs}|$ is larger than a given threshold are excluded from the data set and then included again with $\lambda_{\mathbf{h}} = 0$ when their calculated structure factors fall in the range $0.5 < |F_{\mathbf{h}}|/|F_{\mathbf{h}}^{\rm obs}| < 1.5$. This algorithm introduces a discontinuity into the optimization and may facilitate the search path to switch to other local minima. In the last 50 iterations, however, all reflections in the data set were always used, although this led some trials to be divergent.

(*g*) *Statistics*

The following values are calculated during and after the calculation.

$$R = \sum_{\mathbf{h}}||F_{\mathbf{h}}| - |F_{\mathbf{h}}^{\rm obs}|| \Big/ \sum_{\mathbf{h}}|F_{\mathbf{h}}^{\rm obs}|,$$

$$R_s = \left(\sum_{\mathbf{x}}(\overline{\rho}_{\mathbf{x}} - \rho_{\mathbf{x}})^2 \Big/ \sum_{\mathbf{x}}\rho_{\mathbf{x}}^2\right)^{1/2},$$

$$R_{\rm conv} = \sum_{\mathbf{x}}|(\overline{\rho}_{\mathbf{x}} + \rho_{\mathbf{x}}^{\lambda})/(1 - 2\hat{\rho}_{\mathbf{x}}) - \rho_{\mathbf{x}}| \Big/ \sum_{\mathbf{x}}|\rho_{\mathbf{x}}|.$$

$R_{\rm conv}$ is a measure of the extent to which the constrained optimization has converged, as it goes to zero at the optimum.

Numerical calculations

In order to examine how the present algorithm works, numerical calculations were made using the data observed for 2′-deoxyadenosine (Sato, 1984). Crystal data: $C_{10}H_{13}N_5O_3$, monoclinic, $P2_1$, $a =$

11.298 (2), $b = 10.393$ (2), $c = 4.819$ (1) Å, $\beta = 101.51$ (2)°, $V = 554.5$ (2) Å^3, $Z = 2$, $F(000) = 264$, $B_{overall} = 2.0$ Å^2 from the Wilson plot, $R = 0.038$ for 2224 observed reflections [$\sin\theta/\lambda \le 0.807$ Å^{-1}, $I \ge 2\sigma(I)$]. The same data set as that used in the least-squares refinements was used with the scale factor obtained from the refinements. The value $\overline{A} = 6.611$ was used for (14).

The minimization of the least-squares residual to Sayre's equation was performed under the 'strong' constraints at various resolutions. In all the trials presented in this report, the constraints were satisfied up to $R = 0.0000$ and the convergence was achieved to the extent $0.0002 \le R_{conv} \le 0.0040$. The resulting R_s values are plotted (Fig. 1) as a function of the resolution of the data used and $\overline{B}$ for the density maps that can be considered as corresponding to the correct structure. These values give us some estimates of the extent to which Sayre's equation is accurate in real situations: the error resulting from the overlap of neighbouring atomic densities is very small for $\overline{B} = 6$–8 Å^2 but increases rapidly as $\overline{B}$ increases; the error resulting from the heterogeneity of atoms, on the other hand, becomes more significant when the resolution of the data is increased.

Let us examine some such density maps that demonstrate some notable features of the present method. The first density map (Fig. 2*a*) was obtained when the 2.5 Å data ($s \le 0.200$ Å^{-1}, 43 reflections) were used with $\overline{B} = 6.0$ Å^2. The present method modifies the densities so as to minimize the residual as far as the diffraction data permit. Therefore, when the resolution of the data is lowered and, accordingly, the data become increasingly less restrictive, the density map approaches the ones in which all the peaks have the shape compatible with the postulated scattering factor. In this case, the optimized density map is close to the extreme in the above sense and, consequently, has a very small R_s value of 0.0143. However, this does not mean that the present method can obtain the correct structure with the data of 2.5 Å resolution. In fact, the R_s value is higher than the 0.0048 found for an incorrect structure. This important aspect is described in detail in the following section.

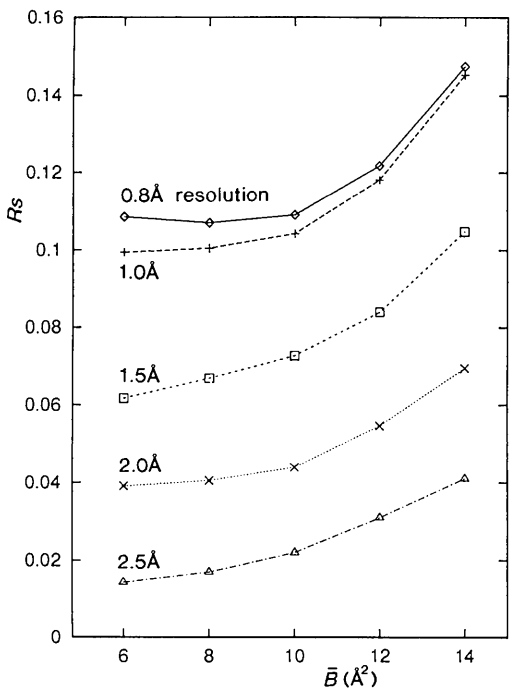

Fig. 1. R_s factors as a function of the resolution of data and $\overline{B}$ plotted for the optimized structures corresponding to the correct structure.

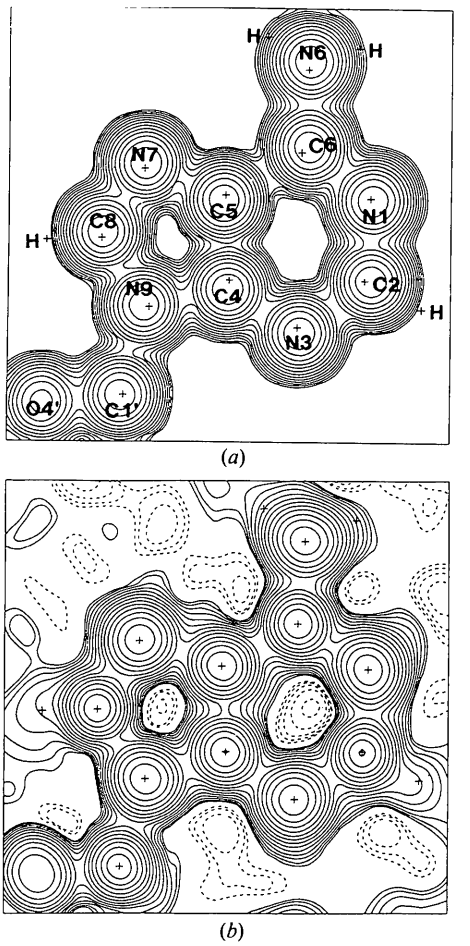

Fig. 2. Optimized densities in the plane of the adenine ring of 2'-deoxyadenosine. (*a*) Densities ($R_s = 0.0143$) obtained at 2.5 Å resolution with $\overline{B} = 6.0$ Å^2. (*b*) Densities ($R_s = 0.1085$) obtained at 0.8 Å resolution with $\overline{B} = 6.0$ Å^2. Contours are drawn at the levels $\pm 0.1 \times 1.5^n$ e Å^{-3} with the positive contours as solid lines, the negative contours as dashed lines. The figures were drawn using *XTAL*3.0 (Hall & Stewart, 1990).

On the other hand, a high R_s value of 0.1085 resulted when the 0.8 Å data ($s \le 0.625$ Å^{-1}, 1152 reflections) were used with $\overline{B} = 6.0$ Å^2. This is because the minimization of the residual was restricted by a wealth of diffraction data. However, the R_s value was definitely lower than that of any incorrect structure. Because of the large residual, the density map obtained (Fig. 2*b*) is far from the extreme and contains many regions where the densities are appreciably negative ($\rho \ge -0.553$ e Å^{-3}). Furthermore, the peak heights are not uniform [in the range 16.7–20.7 e Å^{-3}, compared with 20.0 e Å^{-3} as expected from (14)]. Interestingly, the peak heights of all N and O atoms are lower than those of C atoms. Sayre (1974) obtained a somewhat similar result for Fe and S atoms in rubredoxin.

The use of large $\overline{B}$'s introduces into density maps an additional deformation owing to the overlap of neighbouring atomic densities. However, $\overline{B}$ up to 15.0 Å^2 may be practically usuable and, in some cases, more useful than smaller $\overline{B}$'s. An obvious merit is that coarse grid sizes can be used to save computer time. The other use of larger $\overline{B}$'s is described later. The density map (Fig. 3*a*; 1.8 Å data) shows that the atoms are discernible even with $\overline{B} =$ 12.0 Å^2. However, they are no longer so with $\overline{B} =$ 15.0 Å^2 (Fig. 3*b*; 1.5 Å data); only molecular boundaries are recognizable. In the former map, the peak positions have been shifted from the correct ones to reduce the overlap; the atoms are more separated.

Unusual structures

In the course of trials using initial densities calculated with low-resolution (1.5–3.5 Å) data, several unusual structures were found. They were examined against the 2.0 Å data ($s \le 0.250$ Å^{-1}, 86 reflections) using $\overline{B} = 8.0$ Å^2. Seven different density maps were found to have residuals lower than that of the map corresponding to the correct structure ($R_s = 0.0406$). Among them, three can be considered as 'variants' of the correct structure. (i) In the first map ($R_s =$ 0.0366), one of the ring atoms is appreciably displaced. (ii) The second map ($R_s = 0.0381$) shows a rotation of the six-membered ring. (iii) In the last map (Fig. 4*a*; $R_s = 0.0394$), one of the ring atoms is missing. Clearly, the fact that Sayre's equation is inaccurate for heterogeneous atoms is responsible for the higher residual of the correct structure. However, it is important to understand from these results that the diffraction data of this resolution are unable to distinguish various similar atomic models. This interpretation is in accordance with the fact that, in order to refine the structures of this resolution by least squares, it is necessary to locate stereochemically feasible atomic models and to pose restraints that maintain normal bond distances and angles (Hendrickson, 1985).

On the other hand, the other four density maps with low residuals reveal structures quite different from the correct structure. The first one (Fig. 4*b*; R_s = 0.0195) consists of 34 well resolved peaks, instead of the 18 there should be, with heights in the range 12.1–13.3 e Å^{-3}. Although this structure is apparently incorrect, it has some basis in reality. (i) When the obtained peaks were assigned to C atoms with B = 2.0 Å^2, the observed structure factors within 2.0 Å resolution gave $R = 0.069$. The value can be further reduced to 0.039 if the population parameters are refined (in the range 0.99–1.26). This shows that the structure is quite satisfactory on the basis of the diffraction data. (ii) Provided that a reasonably large $\overline{B}$ is used, the present method can automatically exclude the closest approach of atoms, since this approach causes the overlap of atomic densities,

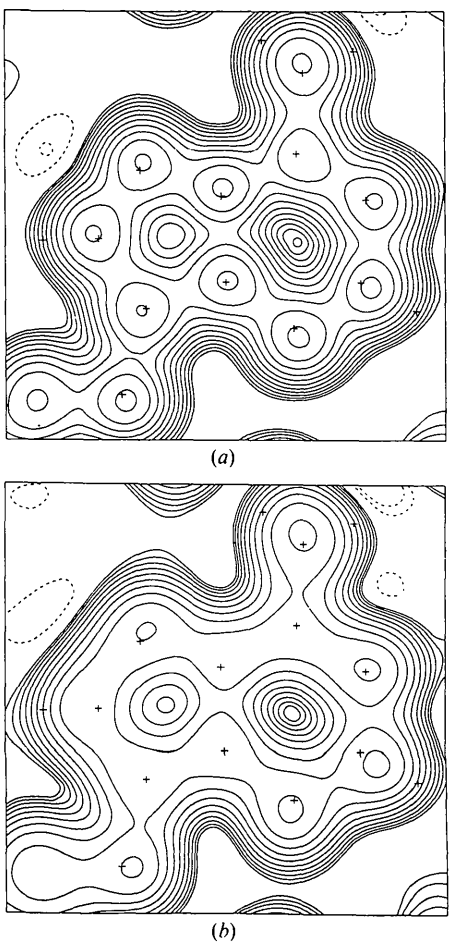

Fig. 3. Optimized densities, which illustrate the use of large $\overline{B}$'s. (*a*) Densities ($R_s = 0.0674$) obtained with $\overline{B} = 12.0$ Å^2 at 1.8 Å resolution. (*b*) Densities ($R_s = 0.1211$) obtained with $\overline{B} =$ 15.0 Å^2 at 1.5 Å resolution. For other details, see Fig. 2.

which is not favoured by the residual. In this case, none of the interatomic distances is shorter than 1.32 Å. Therefore, the structure already satisfies one of the simplest stereochemical requirements. These features are nearly the same for the remaining three density maps ($R_s = 0.0222$, 25 peaks; $R_s = 0.0251$, 24 peaks; $R_s = 0.0286$, 21 peaks).

Importantly, all but one of these unusual structures, including the first three, were no longer more favoured than the correct structure when the 1.8 Å data ($s \leq 0.275$ Å^{-1}, 112 reflections) were used. The very unusual structure shown in Fig. 4(*b*), however, was the most favoured for the 1.8 Å data.

Thus far, the $F(000)$ term has not been included in the calculations. However, if we have a reasonable estimate for it, this estimate can be used as an observed structure factor in the calculation. Calculations were made with the 2.0 Å data for the four structures consisting of too many atoms, for which the calculated $F(000)$ had been 441, 332, 331 and 281, respectively. These were now constrained to be 264. Although the calculations were unsuccessful in reducing the number of peaks, the least-squares residuals of the structures were increased. The first three structures now had R_s values of 0.1250, 0.0628 and 0.0511, respectively, which are appreciably higher than that of the correct structure; the last structure, however, gave $R_s = 0.0333$, which is still lower than that of the correct structure. Thus, the constraint is effective for suppressing the evolution of structures of too many or too few atoms.

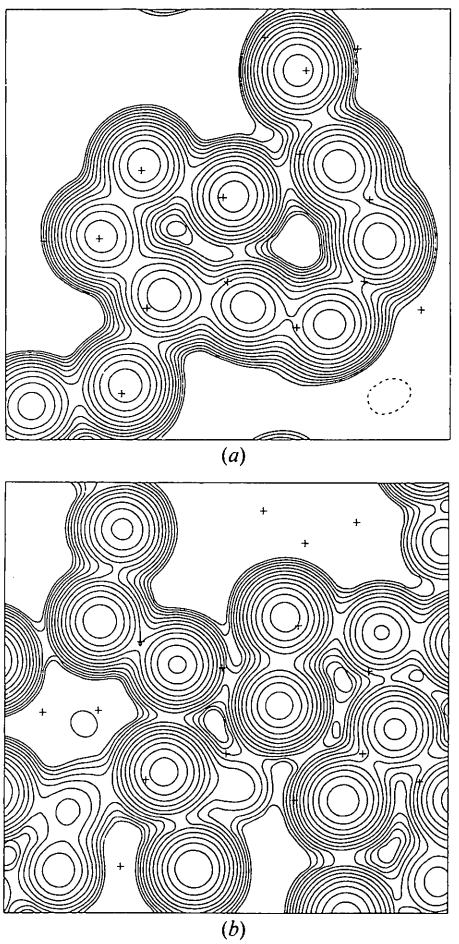

Fig. 4. Unusual structures obtained at 2.0 Å resolution with $\overline{B} = 8.0$ Å^2. (*a*) Densities ($R_s = 0.0394$) showing that one of the ring atoms is missing. (*b*) Densities ($R_s = 0.0195$) consisting of 34 peaks. For other details, see Fig. 2.

Structure refinements

In order to examine whether the present method can be used for structure refinement, various trials were made by starting from incorrect densities. Since the method is essentially a variational one, the radius of convergence is rather small. The following two techniques were found to be useful for recovering the correct structure.

(i) The threshold for the exclusion/inclusion algorithm is set to be as low as twice the mean value of $|\lambda_{\mathbf{h}}|/|F_{\mathbf{h}}|$. This will frequently invoke the exclusion of reflections from the data set and will facilitate the switching of the search path to other local minima, which may be preferable with respect to the residual since, during the exclusion, the residual term is dominant to some extent. A trial starting from one of the unusual structures (21 peaks) recovered the correct structure when the 1.0 Å data were used. However, when the 1.5 Å data were used, the same trial was unsuccessful. This shows that jumping to other minima occurs only when the diffraction data strongly require it.

(ii) Sayre's equation exerts a strong force to normalize peaks, which in turn makes it difficult for existing peaks to disappear or for appearing peaks to evolve. These effects can be to some extent reduced when broad peaks are used. In fact, all of the variant structures described in the preceding section converged to the correct structure when the 1.8 Å data were used with $\overline{B} = 12.0$ Å^2. However, the same trials with $\overline{B} = 8.0$ Å^2 were all unsuccessful.

These techniques expand the radius of convergence to some extent but the calculations performed indicate that, when the data are of low resolution, starting densities should be reasonably close to the correct ones.

Calculations on a small protein

To see how the present method works for more complex structures, calculations were made on crambin (Hendrickson & Teeter, 1981), a small protein of 46 amino acids ($P2_1$, $a = 40.96$, $b = 18.65$, $c =$

22.52 Å, $\beta = 90.77°$). The structure factors used were calculated from the atomic parameters compiled at the Protein Data Bank (Bernstein *et al.*, 1977) but those reflections whose amplitudes were less than $F(000)/200$ were not included in the calculations. To reduce computer time, grid sizes of about 0.30 Å were used with $\overline{B} = 10$ Å^2, although this setting somewhat increased the overlap of neighbouring atomic densities. The optimizaton was performed with reflections in the range 10–1.5 Å resolution, starting from the densities calculated using true phases. The map obtained has $R_s = 0.1227$, which is appreciably higher than the 0.07 obtained for the small molecule under the same condition. This arises from two features common to protein structures. First, the protein contains six S atoms, whose scattering factor is quite different from the one assumed in (14). Second, the distribution of individual temperature factors is very diverse (in the range $3.4 \le B \le 29.0$ Å^2), while $B_{\text{overall}} = 6.0$ Å^2 was used in (13). Accordingly, the optimized density map is subject to distortions: (i) The peaks of the S atoms are very broad in width but low in height. As a consequence of this, the C atoms attached to the S atoms are displaced (Fig. 5*a*). (ii) The atoms of the side chain of Tyr29 (Figs. 5*a* and *b*), which are the most flexible in the protein, show significant displacements, while their peak shapes are exceptionally regular. These two features are those that we found for the small molecule when the resolution was lowered, indicating that the effective resolution for this part is much lower than the nominal one. Regarding this, it should be cautioned that the present method tends to give rise to discrete, but sometimes spurious, peaks in the regions where usual Fourier maps show poor densities.

Nevertheless, in the present case, the general quality of the map is quite satisfactory: all the atoms are identified as resolved peaks of height in the range 7–10 e Å^{-3}, while the backgrounds are within ± 0.5 e Å^{-3}.

Discussion

The minimization of the least-squares residual to Sayre's equation enables one to obtain density maps of atomic resolution without locating atomic models. The quality of the obtained maps compares well with that of the correct ones when the structures are composed only of identical atoms. Even though this is not attainable for real structures of heterogeneous atoms, we have seen for a test structure containing C, N, O and H atoms that the density maps having the lowest residuals well reflect the correct structure when the resolution of the data used is higher than 1.5–1.8 Å. With the data of resolution lower than 2.0 Å, however, we have found many unusual structures having residuals lower than that of the correct structure. Their existence may indicate a limitation inherent in direct methods based on the principle of 'atomicity' in general, since the present method can achieve the requirements of the principle in a direct, rather than probabilistic, exact manner.

The present method has some capability of expanding the radius of convergence but the exclusion/inclusion algorithm is not sufficiently effective for low-resolution structures. To overcome the difficulty of local minima, it would be useful to employ dynamical techniques such as 'simulated annealing' (Kirkpatrick, Gelatt & Vecchi, 1983; Sato, 1994).

A previous method (Barrett & Zwick, 1971) uses Sayre's equation in such a way that the equation itself is capable of refining phases: new refined structure factors $F_{\mathbf{h}}$ can be obtained from the current ones

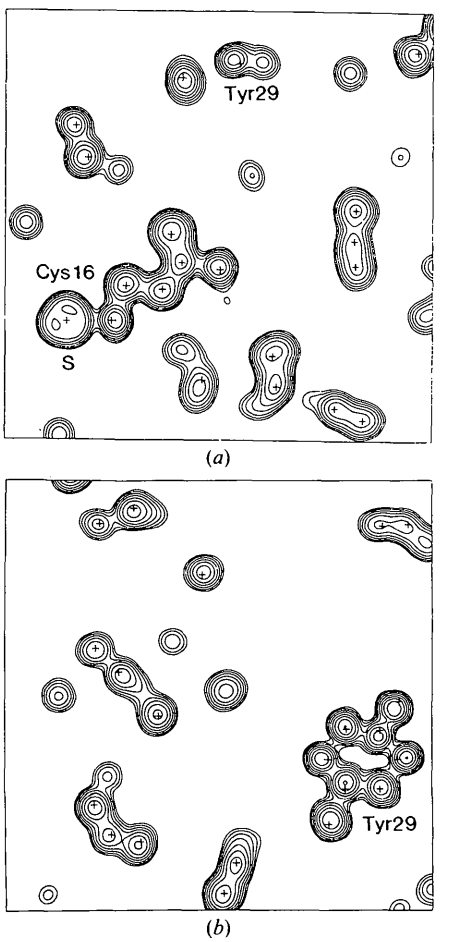

Fig. 5. Densities for crambin optimized at 1.5 Å resolution with $\overline{B} = 10.0$ Å^2. (*a*) Densities in the plane containing the C^α, C^β and S^γ atoms of Cys16. (*b*) Densities in the plane containing the phenyl ring of Tyr29. The crosses indicate the atomic positions of the true structure within 0.5 Å of the plane. Contours are drawn at the levels 0.5×1.5^n e Å^{-3}.

as $(1/V)\Psi_{\mathbf{h}}\Sigma_{\mathbf{k}}F_{\mathbf{h}-\mathbf{k}}F_{\mathbf{k}}$. However, this is not correct because the operation $\psi * \rho^2$, which is equivalent to $(1/V)\Psi_{\mathbf{h}}\Sigma_{\mathbf{k}}F_{\mathbf{h}-\mathbf{k}}F_{\mathbf{k}}$, exaggerates errors in the current densities. The same question points to the current use of the tangent formula (for a review see Woolfson, 1987). As previously shown (Barrett & Zwick, 1971), it is possible to obtain from Sayre's equation

$$\tan \varphi_{\mathbf{h}} = \frac{\sum_{\mathbf{k}} |F_{\mathbf{h}-\mathbf{k}}F_{\mathbf{k}}| \sin (\varphi_{\mathbf{h}-\mathbf{k}} + \varphi_{\mathbf{k}})}{\sum_{\mathbf{k}} |F_{\mathbf{h}-\mathbf{k}}F_{\mathbf{k}}| \cos (\varphi_{\mathbf{h}-\mathbf{k}} + \varphi_{\mathbf{k}})},$$

which is essentially the same as the tangent formula (Karle & Hauptman, 1956). In the light of the argument given above, the phases calculated from this equation are not more correct than the current ones but new more correct phases should be obtained through some process that equalizes the current phases with the calculated ones.

References

Barrett, A. N. & Zwick, M. (1971). *Acta Cryst.* A**27**, 6–11.

Bernstein, F. C., Koetzle, T. F., Williams, G. J. B., Meyer, E. F. Jr, Brice, M. D., Rodgers, J. R., Kennard, O., Shimanouchi, T. & Tasumi, M. (1977). *J. Mol. Biol.* **112**, 535–542.

Cutfield, J. F., Dodson, E. J., Dodson, G. G., Hodgkin, D. C., Isaacs, N. W., Sakabe, K. & Sakabe, N. (1975). *Acta Cryst.* A**31**, S21.

Debaerdemaeker, T., Tate, C. & Woolfson, M. M. (1988). *Acta Cryst.* A**44**, 353–357.

Gull, S. F. & Daniel, G. J. (1978). *Nature (London)*, **272**, 686–690.

Hall, S. R. & Stewart, J. M. (1990). Editors. *XTAL*3.0 *Reference Manual.* Univs. of Western Australia, Australia, and Maryland, USA.

Hendrickson, W. A. (1985). *Mathods Enzymol.* **115**, 252–270.

Hendrickson, W. A. & Teeter, M. M. (1981). *Nature (London)*, **290**, 109–113.

Hestenes, M. R. (1969). *J. Optim. Theor. Appl.* **4**, 303–320.

Hoppe, W. (1963). *Z. Kristallogr.* **118**, 121–126.

Hoppe, W. & Gassman, J. (1964). *Ber. Bunsenges. Phys. Chem.* **68**, 808–817.

Ichikawa, K. (1975). *SICE Trans.* **11**, 180–186. (In Japanese.)

Karle, J. & Hauptman, H. (1956). *Acta Cryst.* **9**, 635–651.

Kirkpatrick, S., Gelatt, C. G. Jr & Vecchi, M. P. (1983). *Science*, **220**, 671–680.

Krabbendam, H. & Kroon, J. (1971). *Acta Cryst.* A**27**, 48–53.

Livesey, A. L. & Skilling, J. (1985). *Acta Cryst.* A**41**, 113–122.

Main, P. (1990). *Acta Cryst.* A**46**, 372–377.

Navaza, J. (1986). *Acta Cryst.* A**42**, 212–223.

Sato, T. (1984). *Acta Cryst.* C**40**, 880–882.

Sato, T. (1992). *Acta Cryst.* A**48**, 842–850.

Sato, T. (1994). In preparation.

Sayre, D. (1952). *Acta Cryst.* **5**, 60–65.

Sayre, D. (1972). *Acta Cryst.* A**28**, 210–212.

Sayre, D. (1974). *Acta Cryst.* A**30**, 180–184.

Sayre, D. (1975). *Crystallographic Computing Techniques*, edited by M. F. C. Ladd & R. A. Palmer, pp. 271–286. New York: Plenum Press.

Shiono, M. & Woolfson, M. M. (1991). *Acta Cryst.* A**47**, 526–533.

Wilkins, S. W., Varghese, J. N. & Lehmann, M. S. (1983). *Acta Cryst.* A**39**, 47–60.

Woolfson, M. M. (1987). *Acta Cryst.* A**43**, 593–612.

Woolfson, M. M. & Yao, J.-X. (1990). *Acta Cryst.* A**46**, 409–413.

Zhang, K. Y. J. & Main, P. (1990). *Acta Cryst.* A**46**, 377–381.

Acta Cryst. (1994). A**50**, 383–391

Novel Treatment of the Experimental Data in the Application of the Maximum-Entropy Method to the Determination of the Electron-Density Distribution from X-ray Experiments

By R. Y. de Vries, W. J. Briels and D. Feil

Chemical Physics Laboratory, University of Twente, PO Box 217, 7500 *AE Enschede, The Netherlands*

(*Received* 6 *September* 1993; *accepted* 17 *November* 1993)

Abstract

The maximum-entropy method (MEM) has been tested on a limited set of noisy Fourier data from a known electron-density distribution (EDD). It is shown that maximizing the entropy of the EDD under the usual condition of fitting the variance of the data set does not necessarily lead to a satisfactory error distribution of the calculated reflections. The MEM property of producing the flattest EDD consistent with the data causes the calculated values of strong reflections to deviate systematically as much as possible from their measured values. Calculated values of strong reflections are usually smaller than their measured values. The use of a novel constraint on the entropy maximization greatly improves the form of the error distribution and also the calculated EDD.

1. Introduction

The common method of extracting the EDD from an incomplete and noisy data set is to fit the data to a